

Stability of convection rolls in a layer with stress-free boundaries

By E. W. BOLTON AND F. H. BUSSE

Department of Earth and Space Sciences and Institute of Geophysics and Planetary Physics,
University of California at Los Angeles

(Received 14 May 1984 and in revised form 6 August 1984)

Steady finite-amplitude solutions for two-dimensional convection in a layer heated from below with stress-free boundaries are obtained numerically by a Galerkin method. The stability of the steady convection rolls with respect to arbitrary three-dimensional infinitesimal disturbances is investigated. Stability is found only in a small fraction of the Rayleigh-number–wavenumber space where steady solutions exist. The cross-roll instability and the oscillatory and monotonic skewed varicose instabilities are most important in limiting the stability of steady convection rolls. The Prandtl numbers $P = 0.71, 7, 10^4$ are emphasized, but the stability boundaries are sufficiently smoothly dependent on the parameters of the problem to permit qualitative extrapolations to other Prandtl numbers.

1. Introduction

Convection in a layer heated from below is typically studied in the case when the layer is bounded by rigid boundaries. This case is readily realized in laboratory experiments, but requires numerical analysis when the study is carried to finite amplitudes of convection. On the other hand, the problem of convection with stress-free boundaries permits several mathematical simplifications in the limit of vanishing amplitudes of convection, and thus has been favoured for the exposition of the mathematical properties of weakly nonlinear convection.

There are more general reasons, however, for the study of convection in the presence of stress-free boundaries. In geophysical and astrophysical applications of convection theory, stress-free boundary conditions are usually more appropriate than no-slip conditions. The variety of different boundary conditions occurring in nature is a strong motivation to study their influence on properties of convection, such as the stability of convection rolls. While convection rolls seem to be the preferred solution independent of the boundary conditions for the velocity field as long as the properties of the fluid layer remain sufficiently symmetric relative to the midplane of the layer, the stability of convection rolls is strongly influenced by the nature of these boundary conditions. It is the main purpose of the present paper to demonstrate the remarkable changes of the stability properties that are introduced when the no-slip conditions are replaced by the stress-free conditions at the boundaries.

The numerical analysis described below has been carried out in conjunction with an analytical treatment of the stability problem in the limit of weakly nonlinear convection (Busse & Bolton 1984, hereinafter referred to as BB84). Because the numerical analysis becomes difficult as the Rayleigh number R approaches its critical value R_c and because the analytical theory loses validity as $R - R_c$ becomes large,

both approaches to the problem complement each other well. Perhaps the most important finding is that convection rolls setting in with the critical wavenumber α_c at $R = R_c$ are always unstable as the Rayleigh number is increased beyond its critical value. For small and for very large Prandtl numbers it can actually be demonstrated that some time-dependent three-dimensional form of convection must replace the two-dimensional convection rolls, since the domain of stable steady solutions vanishes. But at intermediate Prandtl number a finite domain of stable rolls persists for $\alpha < \alpha_c$.

The interesting problem of three-dimensional finite-amplitude convection will not be attacked in the present paper, since it requires different mathematical methods. The results obtained here may be of sufficient interest, however, to stimulate an experimental study of the problem. Such an experiment is indeed possible, as Goldstein & Graham (1969) have demonstrated. Numerical experiments have also become feasible in recent years and some interesting examples of computations of time-dependent three-dimensional convection in the presence of stress-free boundaries have been described by Zippelius & Siggia (1983). As the cost of large-scale computing decreases, larger aspect ratios for the periodicity interval can be realized and the conditions of an infinitely extended layer assumed in the present paper can be approached.

The basic equations and the numerical methods for their analysis are discussed in §2. There is little need for presenting results on steady convection rolls. A fairly complete picture of the properties of steady two-dimensional convection is given by the papers of Veronis (1966) and Moore & Weiss (1973). In §3 the stability of convection rolls in a fluid of high Prandtl number will be discussed. The cases $P = 10^4$ and of water ($P = 7$) will serve as a focus of this discussion. In §4 we shall describe the stability properties in low-Prandtl-number fluids, using air ($P = 0.71$) as an example.

2. Mathematical formulation of the problem

2.1. Basic equations

For the mathematical description of convection rolls and their instabilities in a horizontal layer heated from below, the Boussinesq approximation of the equations of motion and the heat equation will be assumed. For the dimensionless formulation of the problem we introduce the thickness d of the layer as lengthscale, d^2/κ as time scale, where κ is the thermal diffusivity, and $\Delta T/R$ as scale of the temperature, where ΔT is the temperature difference between bottom and top boundaries. The equation of continuity, $\nabla \cdot \mathbf{v} = 0$, can be eliminated by the introduction of the general representation

$$\mathbf{v} = \nabla \times (\nabla \times \lambda \phi) + \nabla \times \lambda \psi \equiv \delta \phi + \epsilon \psi \quad (2.1)$$

for the solenoidal velocity field \mathbf{v} , where λ is the vertical unit vector. By taking the vertical components of the curl and of the curl curl of the Navier–Stokes equation we obtain (2.2*a, b*) for ϕ and ψ :

$$\nabla^4 \Delta_2 \phi - \Delta_2 \theta = P^{-1} \left\{ \delta \cdot [(\delta \phi + \epsilon \psi) \cdot \nabla (\delta \phi + \epsilon \psi)] + \frac{\partial}{\partial t} \nabla^2 \Delta_2 \phi \right\}, \quad (2.2a)$$

$$\nabla^2 \Delta_2 \psi = P^{-1} \left\{ \epsilon \cdot [(\delta \phi + \epsilon \psi) \cdot \nabla (\delta \phi + \epsilon \psi)] + \frac{\partial}{\partial t} \Delta_2 \psi \right\}, \quad (2.2b)$$

$$\nabla^2 \theta - R \Delta_2 \phi = (\delta \phi + \epsilon \psi) \cdot \nabla \theta + \frac{\partial \theta}{\partial t}. \quad (2.2c)$$

Equation (2.2c) is the heat equation for the deviation θ of the temperature from the static distribution. The Rayleigh number R and the Prandtl number P are defined as usual:

$$R = \frac{\gamma g \Delta T d^3}{\nu \kappa}, \quad P = \frac{\nu}{\kappa}, \tag{2.3}$$

where γ is the coefficient of thermal expansion, ν is the kinematic viscosity and $-g\lambda$ is the gravity force. We shall use a Cartesian system of coordinates with the z -coordinate in the λ -direction. The horizontal Laplacian Δ_2 is defined by

$$\Delta_2 \equiv \frac{\partial^2}{\partial x^2} + \frac{\partial^2}{\partial y^2}$$

with respect to this coordinate system. The mathematical formulation of the problem is completed by the conditions

$$\phi = \frac{\partial^2}{\partial z^2} \phi = \frac{\partial}{\partial z} \psi = \theta = 0 \quad \text{at } z = \pm \frac{1}{2} \tag{2.4}$$

at the stress-free boundaries with fixed temperatures.

Schlüter, Lortz & Busse (1965) have shown that the only steady solution of (2.2) that is possibly stable in the neighbourhood of the critical Rayleigh number is the two-dimensional solution describing convection rolls. In order to analyse the stability of convection rolls with respect to arbitrary infinitesimal disturbances in a wide range of Rayleigh numbers, a numerical approximation of the steady two-dimensional solution must be obtained first, and a linear analysis of three-dimensional disturbances must be added in a second step.

2.2. The steady problem

Periodic two-dimensional steady solutions of (2.2) can be obtained by expanding ϕ and θ in terms of orthogonal functions that satisfy the boundary conditions (2.4):

$$\phi = \sum_{m, n=1}^{\infty} a_{mn} \cos m\alpha x \sin n\pi(z + \frac{1}{2}), \quad \theta = \sum_{m=0, n=1}^{\infty} b_{mn} \cos m\alpha x \sin n\pi(z + \frac{1}{2}). \tag{2.5a, b}$$

Since the right-hand side of (2.2b) vanishes there is no vertical component of vorticity associated with the two-dimensional motion. There do not seem to exist periodic solutions without a vertical plane of symmetry, and thus symmetry in x can be assumed. Another simplification arises from the fact that the solutions of interest that exist in the neighbourhood of the critical Rayleigh number belong to the subset of solutions for which the coefficients a_{mn} , b_{mn} vanish whenever $m+n$ is odd. After multiplying (2.2a, c) by $\cos k\alpha x \sin l\pi(z + \frac{1}{2})$ and averaging the result over the fluid layer we obtain nonlinear algebraic equations for the coefficients which can be solved by a Newton-Raphson method. Following earlier authors (Veronis 1966; Clever & Busse 1974), we neglect all coefficients and all equations for which the subscripts k, l satisfy the inequality

$$k+l > N, \tag{2.6}$$

where N is the truncation parameter. A given approximation of the solution can be tested by increasing the truncation parameter by 2. If the convective heat transport

$$H = -R^{-1} \sum_n n\pi b_{0n} \tag{2.7}$$

changes by less than 1 % the solution is considered satisfactory. In the neighbourhood of the critical Rayleigh number well-converged results are obtained for $N = 4$. For larger Rayleigh number $N = 6$ and 8 provide satisfactory approximations. $N = 10$ has been used only at the highest Rayleigh numbers considered in this paper. Since no significant differences have been found in the comparison with the results of earlier authors (Veronis 1966; Moore & Weiss 1973), there is no need to discuss properties of the steady solutions in this paper.

2.3. Stability analysis

For the study of the stability of the steady two-dimensional solutions of the form (2.5) we superimpose infinitesimal disturbances $(\tilde{\phi}, \tilde{\psi}, \tilde{\theta})$ of general three-dimensional form. Since the equations for the disturbances are linear and homogeneous and do not depend explicitly on y and t , an exponential dependence on these coordinates can be assumed. Because the equations are periodic in x the x -dependence of the solution is of the form of a periodic function in x with the same period as the steady solution (2.5) multiplied by the Floquet factor $\exp\{idx\}$,

$$\tilde{\phi} = \exp\{iby + idx + \sigma t\} \sum_{q,p} \tilde{a}_{qp} \exp\{iq\alpha x\} \sin p\pi(z + \frac{1}{2}), \quad (2.8a)$$

$$\tilde{\psi} = \exp\{iby + idx + \sigma t\} \sum_{q,p} \tilde{c}_{qp} \exp\{iq\alpha x\} \cos p\pi(z + \frac{1}{2}), \quad (2.8b)$$

$$\tilde{\theta} = \exp\{iby + idx + \sigma t\} \sum_{q,p} \tilde{b}_{qp} \exp\{iq\alpha x\} \sin p\pi(z + \frac{1}{2}). \quad (2.8c)$$

The summation range is given by $-\infty < q < \infty$, $p \geq 1$; in (2.8b) the summation over p starts with $p = 0$. After inserting (2.8) into the stability equations, multiplying them with the complex conjugates of the expansion functions and taking the average over the fluid layer, we obtain a linear homogeneous system of algebraic equations for the coefficients \tilde{a}_{qp} , \tilde{b}_{qp} , \tilde{c}_{qp} . The growth rate σ is the eigenvalue for this system of equations, and must be evaluated as a function of the parameters b and d . If there exists a growth rate with positive real part for some values of b and d then the steady solution is unstable; otherwise it is stable.

For the actual analysis the system of equations must be truncated. Using the same truncation procedure (2.6) as in the case of the steady solution, we find well-converged results for the growth rate σ in general. The stability boundaries shown in figures 1 and 3 are usually accurate within the line thickness. A simplification of the analysis arises from the property that the disturbances separate into two classes. For class I all coefficients in (2.8) with odd $q+p$ vanish, while for class II all coefficients with even $q+p$ vanish. A further simplification can be obtained in the case $d = 0$ when each class of disturbances splits into two subsets consisting of those disturbances for which $\tilde{\phi}$ and $\tilde{\theta}$ are either symmetric and antisymmetric in x . The function $\tilde{\psi}$ has the opposite symmetry in those two cases. Since many instabilities are characterized by $d = 0$, this symmetry property is of considerable help in analysing the stability problem.

3. Instabilities in high-Prandtl-number fluids

The stability of convection rolls in a fluid layer with stress-free boundaries at infinite Prandtl number has already been studied by Straus (1973). In the present analysis the value $P = 10^4$ has been chosen to approximate the limit of infinite

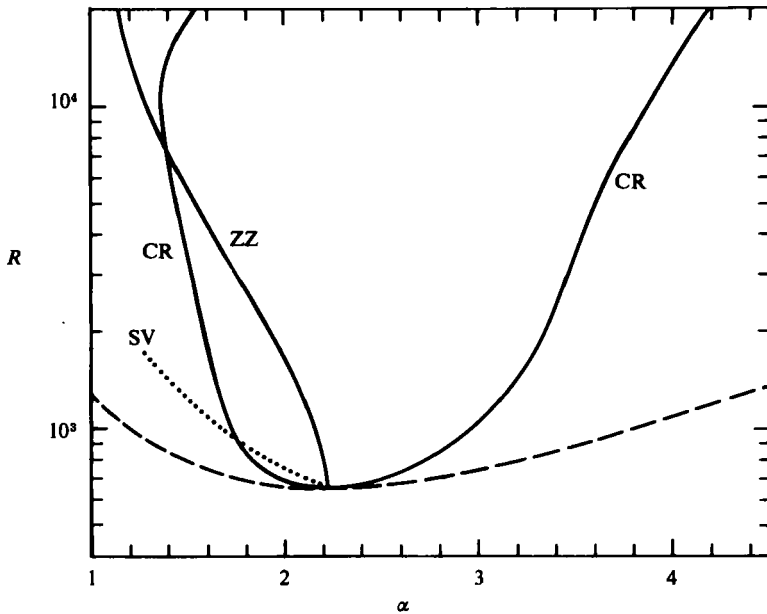


FIGURE 1. Stability boundaries for convection rolls as a function of the Rayleigh number R and the wavenumber α for $P = 10^4$. The symbols CR, ZZ, SV indicate cross-roll instability, zigzag instability and skewed varicose instability respectively. The dashed line describes the Rayleigh number for onset of convection. Because of the onset of the skewed varicose instability above the dotted line, the region of stable rolls is vanishingly small. Since this latter instability becomes negligible in the limit $P \rightarrow \infty$, the effective stability region is actually bounded by the cross-roll instability on the right side and the zigzag and cross-roll instabilities on the left side.

Prandtl number. Except for minor deviations the stability boundaries shown in figure 1 for the onset of the cross-roll and of the zigzag instabilities do indeed agree with the results obtained by Straus. There is a difference, however, introduced by the onset of the monotonic skewed varicose instability. This instability is responsible for the property that the region of stable rolls actually shrinks to a vanishingly small domain for large Prandtl number, as has been deduced in the analytical treatment of BB84. The maximum growth rate of the monotonic skewed varicose instability also decreases with increasing Prandtl number, and approaches zero in the limit $P = \infty$ in the entire domain above the stability boundary. The values of b and d at which the growth rate σ reaches a maximum beyond the stability boundary also decay to zero. The skewed varicose instability thus loses its effect in limiting the stability of convection rolls at infinite Prandtl number, and the major difference between the present results and those of Straus (1972) disappears.

There is little need to characterize the instabilities in detail since this has been done in previous publications devoted to the no-slip boundary case (for a review see Busse 1981). The cross-roll instability corresponds to disturbances of class II that have $d = 0$ and are symmetric in x . The wave number b of the strongest-growing cross-roll mode is close to the critical value $\alpha_c = \pi/\sqrt{2}$ of the wavenumber, indicating the tendency of the cross-roll disturbances to replace the given rolls by rolls at a right-angle with an optimal wavenumber. At Rayleigh numbers of the order 10^4 and higher, the value of b maximizing the growth rate increases similarly as in the case of no-slip boundaries. Since truncation values $N \geq 12$ will be required when the Rayleigh

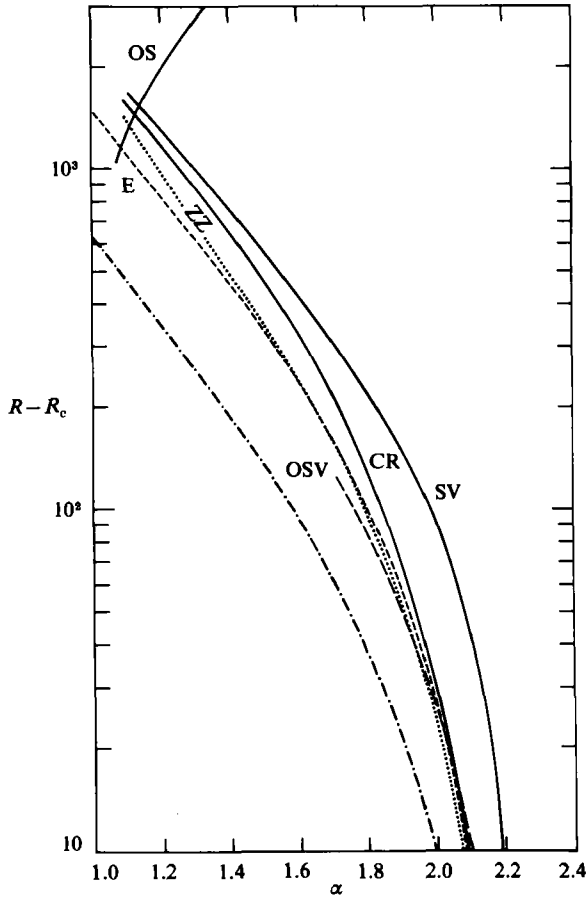


FIGURE 2. Stability boundaries for $P = 7$. In addition to instabilities shown in figure 1, the Eckhaus instability (EC), the oscillatory instability (OS) and the oscillatory skewed varicose instability (OSV) are shown, each of which is growing on the small- α side of the stability boundary. Convection rolls are stable in the region between the onset of the skewed varicose instability towards the right and the cross-roll instability towards the left, except at very low values of $R - R_c$, where the latter instability is replaced by the oscillatory skewed varicose instability. The dash-dotted line indicates the onset of convection.

number exceeds 2×10^4 , we have not pursued the stability boundaries to higher values of R . There is no indication of a transition to bimodal convection caused by a junction of left and right branches of the cross-roll stability boundary as in the case of no-slip boundaries. As has been speculated earlier (Busse 1967), the high heat transport by convection in the presence of stress-free boundaries keeps the thermal boundary layers sufficiently thin to prevent the transition to bimodal convection.

At infinite Prandtl number the zigzag instability prevents the realization of steady rolls with a wavenumber α less than α_c in the neighbourhood of $R = R_c$. This result of Schlüter *et al.* (1965) must be modified at finite Prandtl number, as was pointed out by Siggia & Zippelius (1981). Owing to the finite $\tilde{\psi}$ -component of the disturbance, the zigzag instability becomes less dangerous as the Prandtl number decreases, and the criterion for instability assumes the form

$$R - R_c \leq 18\pi^2(\alpha - \alpha_c)^2 (1 + f(P)), \quad \alpha < \alpha_c, \quad (3.1)$$

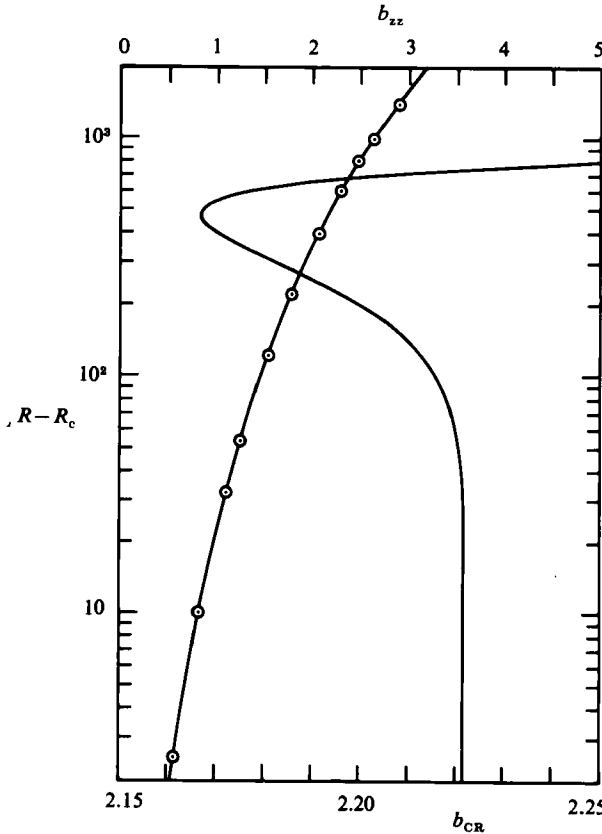


FIGURE 3. The wavenumbers b_{CR} (lower scale) and b_{ZZ} (upper scale, curve marked by circles) of the disturbances of maximum growth near the stability boundary for the cross-roll and the zigzag instabilities in the case $P = 7$.

with
$$f(P) = P^2/4(1 + P) \tag{3.2}$$

in the neighbourhood of the critical Rayleigh number (Siggia & Zippelius 1981; BB84). The criterion for instability with respect to the cross-roll instability is of the same form (3.1), but with a different function $f(P)$ (Busse 1971),

$$f_{cr}(P) = \left[0.42084 + \frac{0.25372}{P} + \frac{0.15224}{P^2} \right]^{-1}, \tag{3.3}$$

and without the restriction $\alpha < \alpha_c$. At the Prandtl number $P = 9.832$ the right-hand side of the inequality (3.1) is the same for zigzag and cross-roll instabilities, and for lower Prandtl number the cross-roll instability is more dangerous than the zigzag instability.

The latter property is evident in figure 2, which shows various stability boundaries in the case of water ($P = 7$). The region of stable convection rolls is bounded mainly by the cross-roll instability from below and by the skewed varicose instability from above. But in the region near the critical Rayleigh number the stability properties are more complex than we have discussed so far. A new instability becomes noticeable which was first described by BB84 and has been called the oscillatory skewed varicose instability in distinction to the monotonically growing ordinary skewed varicose

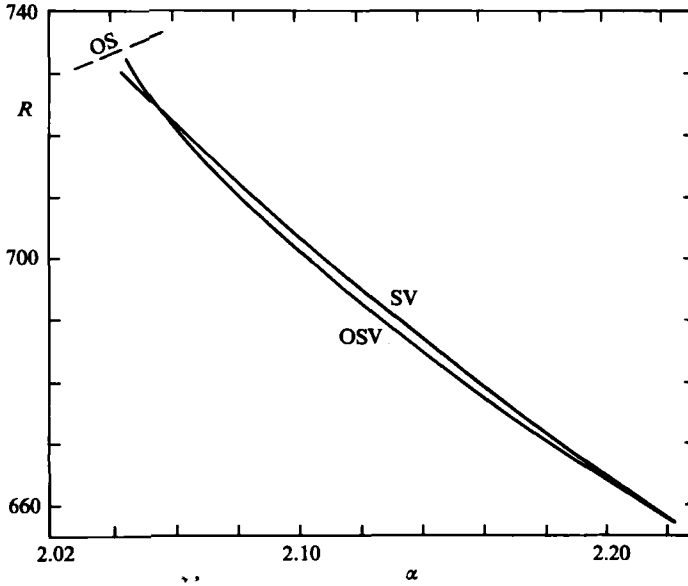


FIGURE 4. Stability boundaries for convection rolls in air ($P = 0.71$). Only boundaries corresponding to the onset of the oscillatory (OS), the skewed varicose (SV) and the oscillatory skewed varicose instability (OSV) are shown. Rolls are stable only within the thin region bounded by the latter two instabilities.

instability mentioned above. Both skewed varicose instabilities yield stability boundaries with a linear relationship between $R - R_c$ and $\alpha - \alpha_c$ in the neighbourhood of the critical Rayleigh number, such that the criterion for instability can be written in the form

$$\pm [R - R_c - (\alpha_c - \alpha) \alpha g^{(\pm)}(P)] > 0, \quad \alpha < \alpha_c, \quad (3.4)$$

with the upper sign applying in the monotonic case and the lower sign in the oscillatory case. While the function $g^{(+)}(P)$ is actually independent of the Prandtl number, $g^{(+)}(P) = \frac{10^2}{7}\pi^2$, the function $g^{(-)}(P)$ strongly decreases with the increasing Prandtl number (see expression (3.17) of BB84).

A fourth instability which becomes important in bounding the region of stable convection rolls is the oscillatory instability, which was first studied by Busse (1972). While the section of the stability boundary corresponding to this instability is minute, it is responsible for restricting the Rayleigh-number range for which steady convection rolls can be realized in the range $0.8 \lesssim P \lesssim 10$.

As has been noted by Siggia & Zippelius (1981), the growth rate of the zigzag instability reaches a maximum at a wavenumber b which increases proportionally to $(\alpha_c - \alpha)^{\frac{1}{2}}$ in the neighbourhood of the critical Rayleigh number. This increase becomes amplified at higher Rayleigh numbers as shown in figure 3, such that the preferred value of b exceeds α_c for Rayleigh numbers above twice the critical value R_c . The preferred value b of the cross-roll instability stays close to the critical wavenumber α_c for low Rayleigh number, as has already been mentioned in connection with the results for $P = 10^4$. Around $R = 10^3$ the preferred wavenumber b_{\max} reaches a minimum, however, and increases relatively sharply at higher Rayleigh numbers. Since the stability boundary is rather smooth throughout this regime, the cause for the variation of b_{\max} is not clear.

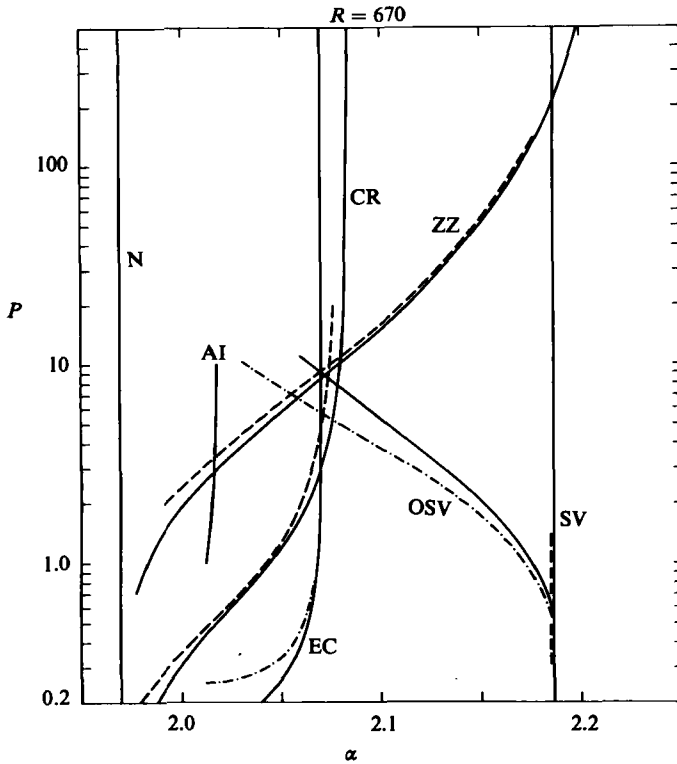


FIGURE 5. The stability boundaries as a function of the wavenumber and the Prandtl number P for $R = 670$. The symbols refer to the various instabilities as explained in the preceding figures. The dashed lines correspond to the analytical expressions of BB84. The amplitude instability (AI) corresponds to growing sinusoidal variation of the amplitude of the rolls along their axis. This instability that does not bound the region of stable rolls corresponds to expression (3.6*b*) of BB84. Convection solutions exist to the right of curve N. Growing disturbances exist in the left of all stability boundaries except for the skewed varicose boundary.

4. Instabilities in low Prandtl-number fluids

A remarkable property of the monotonic skewed varicose instability is that its stability boundary is independent of the Prandtl number. In the limit of small amplitudes of convection this feature is apparent from the analytical expression of BB84. But even at the largest Rayleigh numbers considered in this study a variation of the stability boundary with Prandtl number could not be detected. We have not been able yet to prove this result in general. A major part of the stability boundary for convection rolls is thus invariant as the Prandtl number changes, and the main variations occur at the boundary limiting the stability region of steady rolls on the low-wavenumber side.

As the Prandtl number decreases from the value 7 of figure 2, the cross-roll boundary shifts towards lower wavenumbers, while the opposite effect occurs in the case of the oscillatory skewed varicose instability. As the Prandtl number of air ($P = 0.71$) is reached, the lower boundary of the stability region corresponds entirely to the onset of the latter instability as shown in figure 4. Because of the intersection of the boundaries of the two skewed varicose instabilities, the oscillatory instability no longer bounds the stability region for Prandtl numbers less than about 0.8. As

the Prandtl number drops below 0.71 the region of stable rolls diminishes rapidly until it disappears completely at $P = 0.543$.

The dependence of the stability region on the Prandtl number for $R = 670$ is illustrated in figure 5, which demonstrates how various instabilities replace each other in providing the stability boundary towards low values of α . The boundary towards high values α is given by the monotonic skewed varicose instability independent of the Prandtl number. Because the Rayleigh number used in the graph exceeds the critical value only by about 2%, one expects that the analytical results BB84 should yield a good approximation. The comparison between solid and dashed lines of figure 5 confirms this expectation. The sense of the deviation of the analytical formulas from the numerical results may be used to infer the effects of higher-order terms neglected in the analytic perturbation formulation. In particular, it can be seen that the crossover point from the zigzag to cross-roll instability discussed in §3 is relatively independent of the amplitude of convection.

In testing the computer code developed for the stability analysis a small discrepancy with a result for the oscillatory instability of Busse (1972) was discovered. The formula (3.18) for the critical amplitude A_1 of convection in that paper should be

$$A_1 = 1.114 \quad \text{instead of} \quad A_1 = 1.215. \quad (4.1)$$

The discrepancy was independently discovered by B. F. Edwards and A. L. Fetter (1983, private communication), who traced it to the incorrect appearance of a factor 3 multiplying π^2 in the first line of (3.16) and the fact that $\frac{1}{16}$ should be replaced by $\frac{1}{8}$ in the second line of the same equation. Because the effect of this error on the critical amplitude A_1 is relatively small, the error was not discovered when the analytical results were compared with the independent approximate Galerkin analysis, which is also reported in the paper of Busse (1972).

5. Concluding remarks

The stability of steady convection rolls is even more restricted at finite amplitudes than might have been expected on the basis of the small-amplitude result of BB84. The wavenumber range for which rolls are stable never exceeds more than about 10% of the mean wavenumber, and the Prandtl-number range for which stable steady rolls exist decreases as the Rayleigh number increases from its critical value. The maximum Rayleigh number for which steady rolls can be realized is also relatively low. We have not made an effort to determine it accurately. But it is unlikely to be much larger than about 3 times the critical value, and will be reached for a Prandtl number somewhat in excess of that for water. This maximum Rayleigh number is realized when the zigzag instability replaces the oscillatory instability at the upper part of the stability region by intersecting with the skewed varicose stability boundary.

The limit of infinite Prandtl number must be excepted from the above statements. The property that the skewed varicose instability vanishes in that limit appears to be unique in the stability theory of convection rolls. In the case of rigid boundaries the growth rate of the skewed varicose instability also decays with increasing Prandtl number; but at high Prandtl numbers it is preceded by the transition to bimodal convection. A measure of the strength of the skewed varicose instability is given by the increase of the maximum growth rate σ_m beyond the stability boundary, $\alpha > \alpha_{sv}$,

at a given value of R . According to the analytical theory of BB84, the growth rate σ can be written in the form

$$\sigma = bs_1 \left(s_2(\alpha - \alpha_{sv}) - \frac{b^2}{d^2} \right)^{\frac{1}{2}} - \sigma_{02} d^2 + \dots \quad (5.1)$$

at a given value of the Rayleigh number, where contributions to σ of the order b^2 and d^3 have been neglected. The constants s_1 and s_2 are independent of the Prandtl number P if the different timescale used on the present paper is taken into account; but σ_{02} has not been evaluated in BB84. The numerical computations indicate that σ_{02} grows like $P^{\frac{2}{3}}$ for large P . Using this information, we deduce from (5.1) that maximum growth rate σ_m and the maximizing values d_m and b_m of d and b exhibit the approximate dependences

$$\sigma_m \propto (\alpha - \alpha_{sv})^2 P^{-\frac{2}{3}}, \quad d_m \propto (\alpha - \alpha_{sv}) P^{-\frac{1}{3}}, \quad b_m \propto (\alpha - \alpha_{sv})^{\frac{1}{2}} P^{-\frac{1}{3}} \quad (5.2)$$

for large Prandtl number and small values of $\alpha - \alpha_{sv}$. The numerical results show that the relationships (5.2) do not only hold in the neighbourhood of the critical Rayleigh number, but appear to be valid at higher Rayleigh numbers as well.

A large number of numerical results have been obtained for Rayleigh numbers close to the critical in order to test the predictions of the analytical theory of BB84. Agreement within the expected numerical accuracy has been obtained in all cases. Because of the relative simplicity of the analytical expressions given in BB84 there is no need to present numerical results for slightly supercritical Rayleigh numbers. In particular, the approximate form of the disturbed rolls can be inferred from the expressions given in BB84. For larger Rayleigh numbers the dependence of the stability boundary on the Prandtl number can be inferred at least in a rough sense by interpolation between the few cases on which the analysis of this paper has been focused.

The research reported in this paper has been supported by the Atmospheric Sciences Section of the U.S. National Science Foundation. Computer funds have been supplied by the UCLA College of Letters and Science. We wish to thank Dr R. M. Clever and Mr A. Quintanar, who have helped us in some aspects of the numerical analysis.

REFERENCES

- BUSSE, F. H. 1967 On the stability of two-dimensional convection in a layer heated from below. *J. Math. & Phys.* **46**, 140–150.
- BUSSE, F. H. 1971 Stability regions of cellular fluid flow. In *Instability of Continuous Systems* (ed. H. Leipholz), pp. 41–47. Springer.
- BUSSE, F. H. 1972 The oscillatory instability of convection rolls in a low Prandtl number fluid. *J. Fluid Mech.* **52**, 97–112.
- BUSSE, F. H. 1981 Transition to turbulence in Rayleigh–Bénard convection. In *Hydrodynamic Instabilities and the Transition to Turbulence* (ed. H. L. Swinney & J. P. Gollub), pp. 97–137. Springer.
- BUSSE, F. H. & BOLTON, E. W. 1984 Instabilities of convection rolls with stress-free boundaries near threshold. *J. Fluid Mech.* **146**, 115–125.
- CLEVER, R. M. & BUSSE, F. H. 1974 Transition to time-dependent convection. *J. Fluid Mech.* **65**, 625–645.
- GOLDSTEIN, R. J. & GRAHAM, D. J. 1969 Stability of a horizontal fluid layer with zero shear boundaries. *Phys. Fluids* **12**, 1133–1137.

- MOORE, D. R. & WEISS, N. O. 1973 Two-dimensional Rayleigh-Bénard convection. *J. Fluid Mech.* **58**, 289-312.
- SCHLÜTER, A., LORTZ, D. & BUSSE, F. 1965 On the stability of steady finite amplitude convection. *J. Fluid Mech.* **23**, 129-144.
- SIGGIA, E. D. & ZIPPELIUS, A. 1981 Pattern selection in Rayleigh-Bénard convection near threshold. *Phys. Rev. Lett.* **47**, 835-838.
- STRAUS, J. M. 1972 Finite amplitude doubly diffusive convection. *J. Fluid Mech.* **56**, 353-374.
- VERONIS, G. 1966 Large-amplitude Bénard convection. *J. Fluid Mech.* **26**, 49.
- ZIPPELIUS, A. & SIGGIA, E. D. 1983 Stability of finite-amplitude convection. *Phys. Fluids* **26**, 2905-2915.